USGS
science for a changing world

High-Resolution Seismic Imaging for Environmental and Earthquake Hazards Assessment at the Raychem Site, Menlo Park, California

by Rufus D. Catchings, Elba Horta, Mark R. Goldman, Michael J. Rymer, and Thomas R. Burdette[1]

Open-File Report 98-146

1998

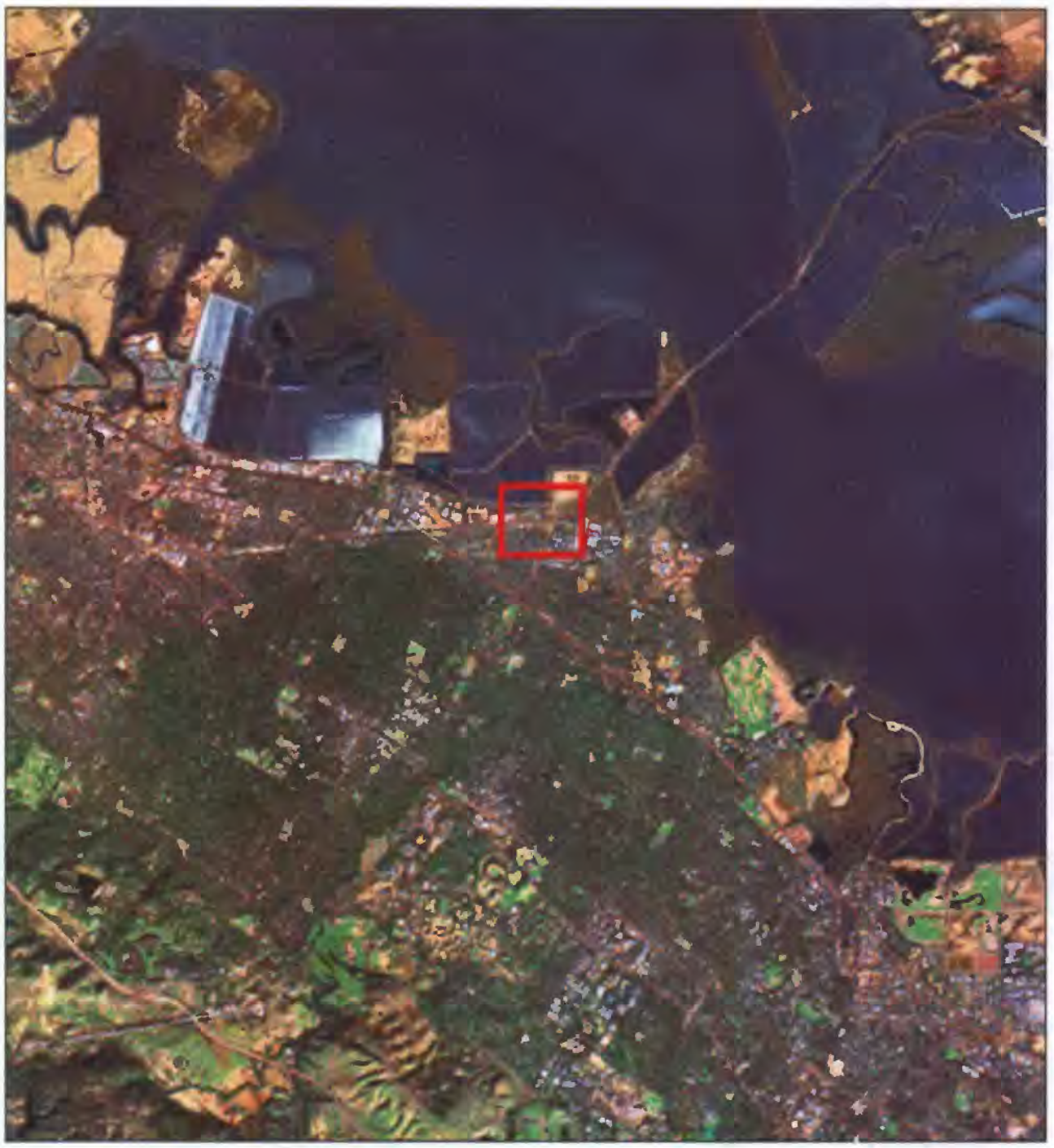

U.S. GEOLOGICAL SURVEY

[1]Menlo Park, California

Table of Contents

List of Tables

List of Figures

Introduction

In this report, we present acquisition parameters, data, and an interpretation of seismic data from a high-resolution seismic imaging investigation at the Raychem Corporation site in Menlo Park, California, located along the southwestern end of the San Francisco Bay (Fig. 1a, b). The data were acquired by the U. S. Geological Survey in May, 1997 as a joint investigation between the USGS Western Earthquake Hazards Team, the USGS Water Resources Division, and Raychem Corporation. The objectives of the seismic investigation were: (1) to determine practicality of using high-resolution seismic imaging to locate subsurface sand-channel aquifers that transport chemical contaminants, (2) to obtain velocity measurements of near-surface sediments to aid in earthquake hazard assessments, and (3) to investigate possible shallow faults near the San Francisco Bay margin.

In many geological environments, seismic imaging can be a cost effective method of characterizing the subsurface for purposes of hazards mitigation. At the Raychem site, subsurface sand-channel aquifers may transport contaminants from the Raychem site toward the San Francisco Bay, but the channels are apparently highly sinuous. The sinuous nature of the subsurface aquifers make it difficult to determine where to place boreholes so that they will intersect the contaminant-bearing aquifers at depth. Although the channels could be approximately located by greatly increasing the density of boreholes, drilling such a great number of holes is costly and increases the risk of contaminating deeper aquifers by puncturing the underlying aquitards. High-resolution seismic imaging provides a means of more strategically identifying favorable drill sites and provides stratigraphic information that can be used to avoid breaching subsurface aquitards..

For purposes of earthquake hazards assessment, we used the seismic data to make high-quality measurements of the shallow (<30 m) seismic velocity structure associated with the San Francisco Bay sediments. Numerical models of the strength of shaking can be developed on the basis of measured compressional and shear-wave velocities and structure. Studies have shown that unconsolidated sediments amplify ground motions from earthquakes (Borcherdt, 1970; Borcherdt et al., Gibbs, 1975), and in unconsolidated and saturated sediments, the ground is susceptible to liquefaction. Few measurements of the shallow velocity structure near the San Francisco Bay are available, and most of the available velocity measurements are determined from borehole measurements. However, borehole velocity measurements provide velocities that may only be specific to the site near each borehole. Surface measurements of the type presented here, however, provide both laterally varying velocities and structure.

We also used the high-resolution seismic images to search for possible earthquake faults in the sediments above the basement rocks.

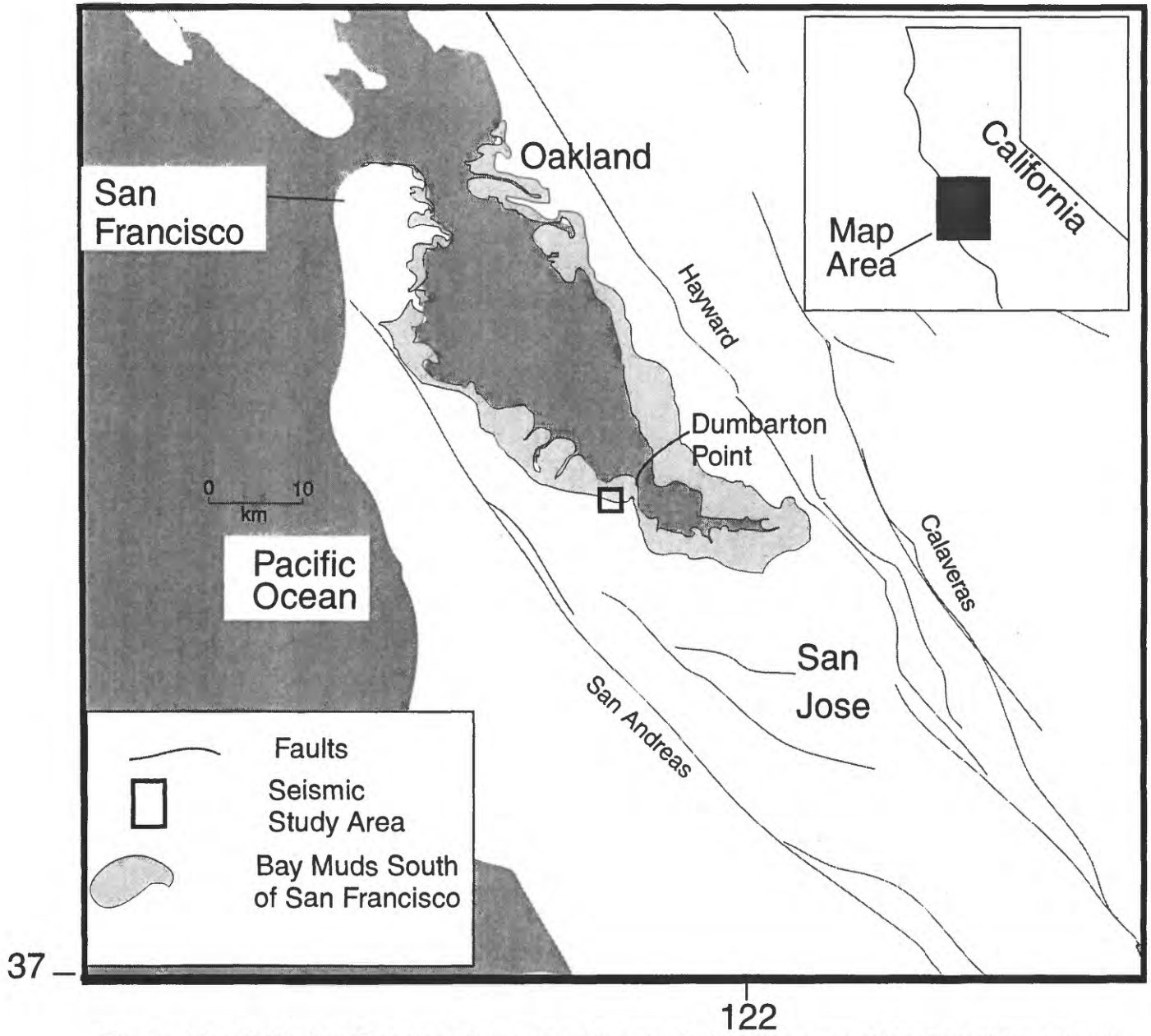

Fig. 1a Map of the San Francisco Bay area with major faults. The general location of our seismic investigation is shown with a black rectangle

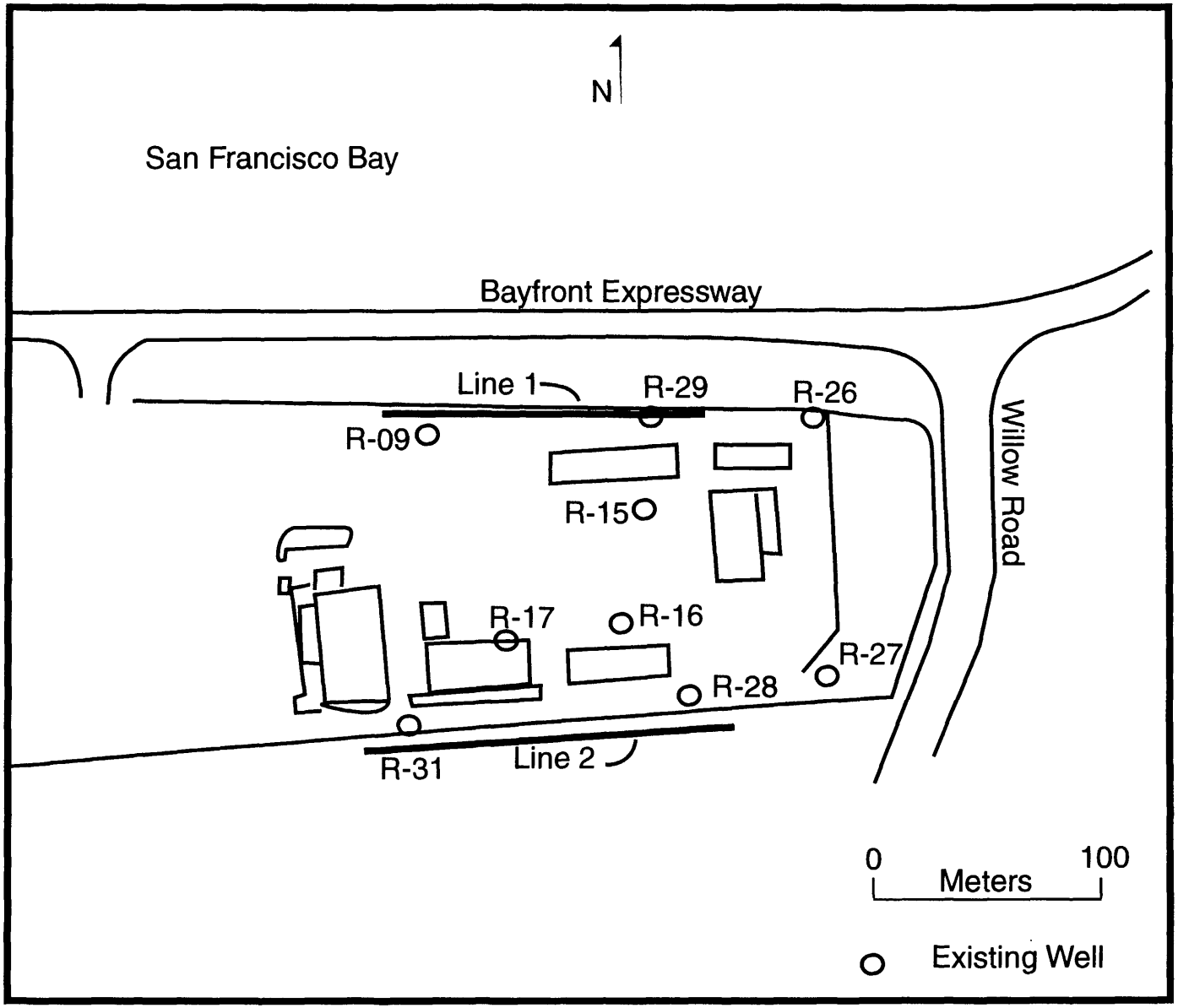

Fig. 1b. The eastern end of the Raychem site, locations of seismic lines 1 and 2 (bold lines), and existing wells (R-#) relative to Willow Road and the Bayfront Expressway.

Local Geology

The San Francisco Bay area is a tectonically active region that lies between two major right-lateral, strike-slip faults, the San Andreas and Hayward faults (Fig. 1a). Due to fault-normal compression along the San Andreas and Hayward faults, mountain ranges parallel the San Francisco Bay on each side, and the lower-lying area between the two ranges is covered by Quaternary alluvium deposits and Holocene bay muds (Lajoie, in Borhcerdt and others, 1975). At the Raychem site, the surficial geology consists of artificial fill and Holocene estuarine bay muds. These surficial deposits are underlain by Quaternary alluvium (sand, clay, silty clay, and sandy gravel) and Pleistocene marine and continental (sand, sandy silt, and gravel) deposits (Borcherdt and Glassmoyer, 1994).

A borehole at nearby Dumbarton Point (Fig. 1a; Table 1) shows that the upper 180 m of the subsurface consists of a series of muds, clays, sands, and gravels that overlie basement rocks consisting of brown sandstone and graywacke (Warrick, 1974). Such layered sediments with high impedance contrasts are ideal for imaging laterally varying stratigraphic sequences more than about 1 m thick.

Table 1. Stratigraphy from 180-m-deep borehole at Dumbarton Point (from Warrick 1974).

Depth Range	Stratigraphy	Description
0-2m	Mud	Younger Bay Mud
2m-12m	Soft Clay	Younger Bay Mud
12-20	Clay	Older Bay Sediments
20-22	Sand	Older Bay Sediments
22-30	Clay	Older Bay Sediments
30-32	Sand	Older Bay Sediments
32-39	Clay	Older Bay Sediments
39-55	Soft Clay	Older Bay Sediments
55-62	Gravel	Older Bay Sediments
62-78	Clay	Older Bay Sediments
78-80	Sand	Older Bay Sediments
80-82	Gravel	Older Bay Sediments
82-104	Stiff Clay	Older Bay Sediments
104-106	Sand and Gravel	Older Bay Sediments
106-155	Clay and Silt	Older Bay Sediments
155-157	Sand	Older Bay Sediments
157-170	Hard Clay & Silt	Older Bay Sediments
170-172	Sand and Silt	Older Bay Sediments
172-180	Clay and Silt	Older Bay Sediments
180-185	Sand and Clay	Older Bay Sediments
185-190	Brown Sandstone and greywacke	Bedrock

Seismic Survey

Data Acquisition

The US Geological Survey acquired two high-resolution seismic reflection/refraction profiles at the Raychem site in Menlo Park, California during May 1997 (Fig. 1b). Line 1 was oriented approximately east-west, adjacent the Raychem property line and parallel to the Bayfront expressway. Line 1 consisted of a linear array of about 60 seismic sources. The seismic sources were recorded on an array of 60 geophones spaced about 2 m apart. Well logs from two wells (R-29 and R-09) along line 1 provided stratigraphic data (Fig. 1b). We used a similar geometrical setup for line 2, which was located approximately 120 m south of line 1, subparallel to line 1. Two wells (R-28 and R-31) were located approximately 12 m north of line 2, which was within a drainage south of the Raychem property. The drainage was approximately 1.5 to 2 m lower in elevation than the ground surface at wells R-28 and R-31. We acquired both lines 1 and 2 during periods of high traffic volume on Willow Road and the Bayfront expressway; however, field tests showed that nearly all of the noise caused by the traffic was below about 35 Hz. Therefore, the cultural noise did not significantly affect the seismic data of interest.

The data were recorded on a Geometrics RX-60 seismograph using vertical-component Mark Products 40-Hz geophones. Each geophone was spaced approximately two meters apart. Seismic sources were generated by 8-gauge, 300-grain shotgun blanks fired at a depth of approximately 0.5 m. Seismic sources were fired at two-meter intervals, adjacent to the geophones (see Appendices A and B). The data were recorded for 4 seconds without filters at a sampling rate of 0.5 ms. To obtain 24 fold on the ends of the recording array, as many as 11 shots were fired off the ends of the arrays. A summary of the acquisition parameters are shown in Table 2.

Table 2. Acquisition parameters for Raychem seismic profiles. Distances are relative to first shot point at starting end of line.

Line #	Orientation	Length of Geophone Line (m)	Length of Shot Point Line (m)	No. of Shots	No. of CDP's	Maximum Fold
1	E-W	118.08	141.83	75	138	58
2	E-W	118.59	165.84	84	156	60

Shot and Receiver Locations

All shots were recorded on each seismic profile by 60 live channels. Individual shots were co-located with a geophone and were laterally offset

from the geophone by approximately 1 m. Additional shotpoints were extended off the ends of each recording array to increase the fold at the ends of the recording arrays. Shotpoints and geophones were surveyed using a measuring tape prior to acquiring the data, and after acquiring the data, each shotpoint and geophone was re-surveyed using an electronic distance meter (total station). Accuracies of the surveying device are approximately 1 cm, but the actual locations are likely to be on the order of about 10 cm due to surveyor error.

Line 1:

Details of the seismic survey geometry is presented here for the benefit of anyone wishing to reprocess the seismic data or to estimate possible artifacts caused by the geometrical configuration. Geophone distances (X) are relative to the first geophone, and geophone elevations (Z) are relative to the topographically lowest geophone location along line 1 (Fig. 2). Geophone elevations along line 1 vary by no more than 19 cm along the ~118 m distance of the line. Horizontal variations (Y) are relative to a line connecting the first and last geophone.

A total of 75 shots were recorded on line 1. Shotpoint distances (X) are relative to the first shotpoint, which was off the end of the recording array, and elevations are relative to the topographically lowest shotpoint along line 1 (Fig. 3). Shotpoint elevations vary by less than 19 cm along line 1. Horizontal variations (Y) are relative to a line connecting the first and last shotpoint. Individual shotpoints vary from a straight line by no more than 28 cm along the ~142 m distance of line 1.

Line 2:

The geophone recording array along line 2 was similarly configured as that of line 1. The total length of the recording array was approximately 119 m, with a total of 60 geophones spaced approximately 2 m apart. Geophone distances (X) and elevations (Z) for line 2 are shown in figure 4. Horizontal variations (Y) of the array of geophones from a straight line were less than 25 cm.

Due to fewer physical obstructions along line 2, we recorded a total of 84 shots. Shotpoints were spaced approximately 2 m apart, and the total distance from shotpoint 1 to shotpoint 84 was approximately 165 m. Shotpoint elevations varied by less than 25 cm (Fig. 5). Horizontal variations (Y) varied no more than 26 cm.

Seismic Processing

The shots were recorded in the field on the hard disk of the Geometrics RX-60 seismograph in SEG-D format. The resulting data were later transferred to digital audio tapes for permanent storage in SEG-Y format. The seismic reflection data were processed using Promax interactive analysis software.

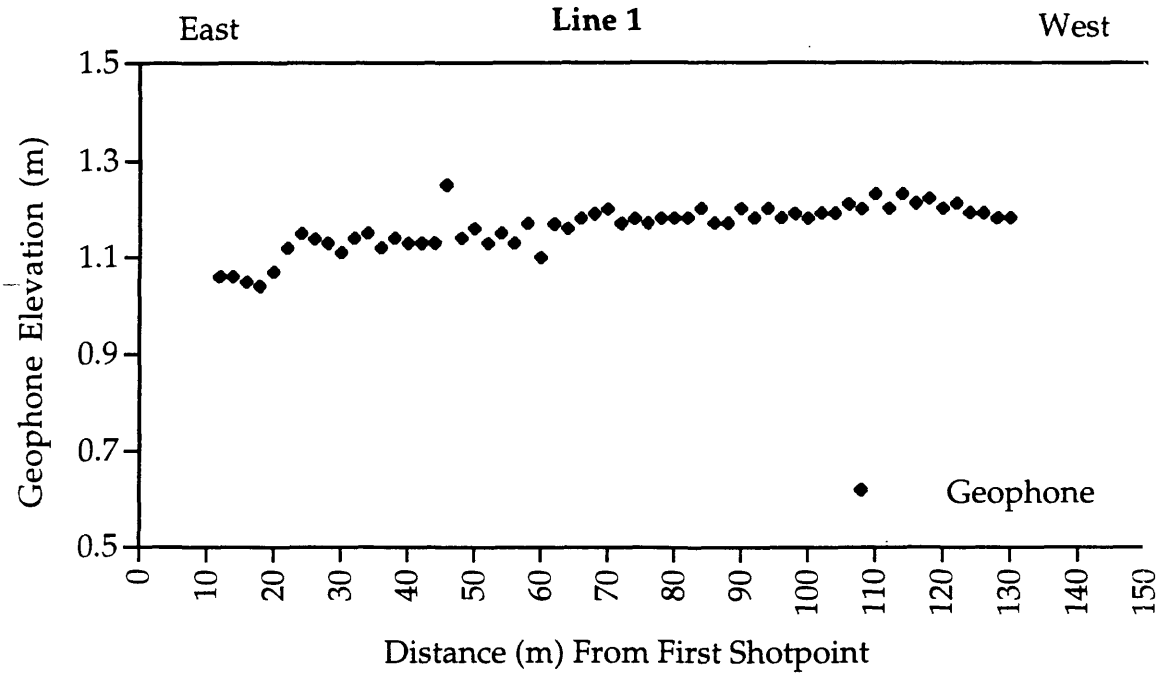

Fig. 2a. Geophone elevations (relative to the topographically lowest geophone) versus distance

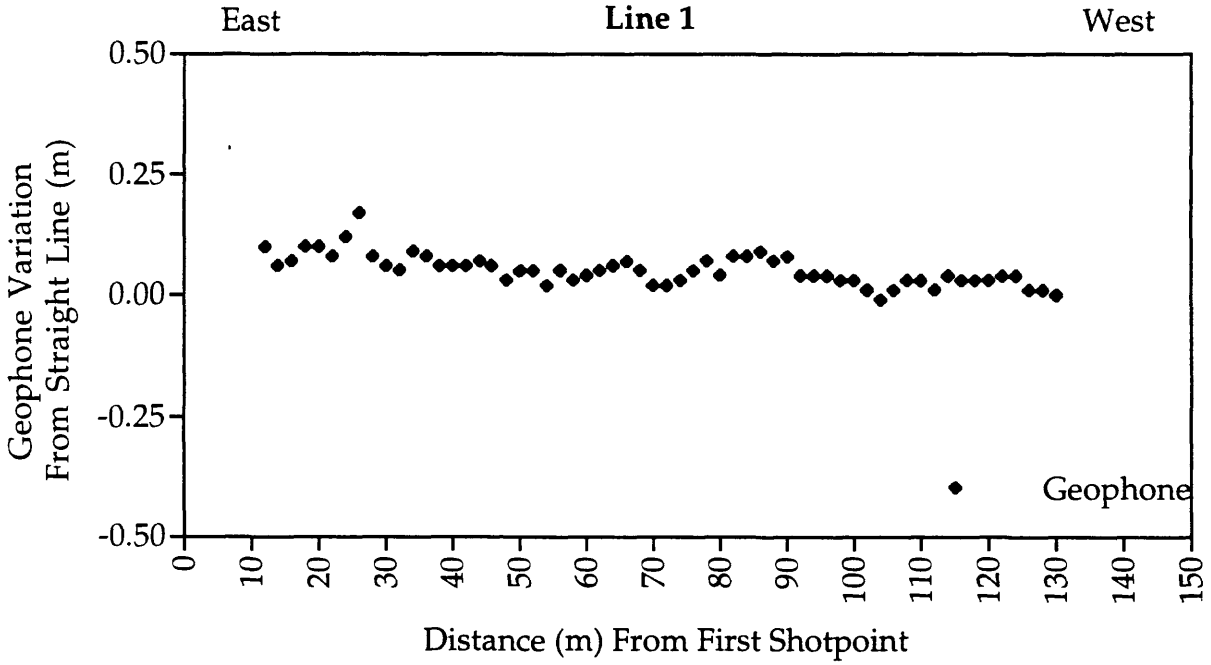

Fig. 2b. Geophone variation from a straight line connecting the end points

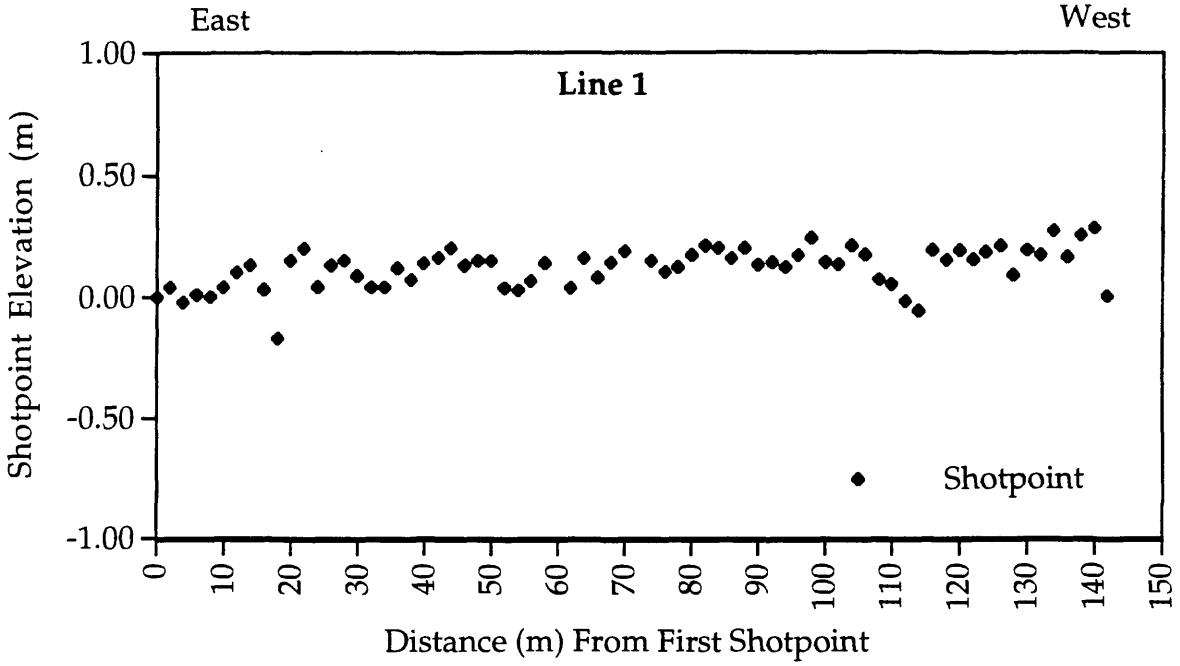

Fig. 3a. Shotpoint elevations (relative to the topographically lowest shotpoint along the line) versus distance.

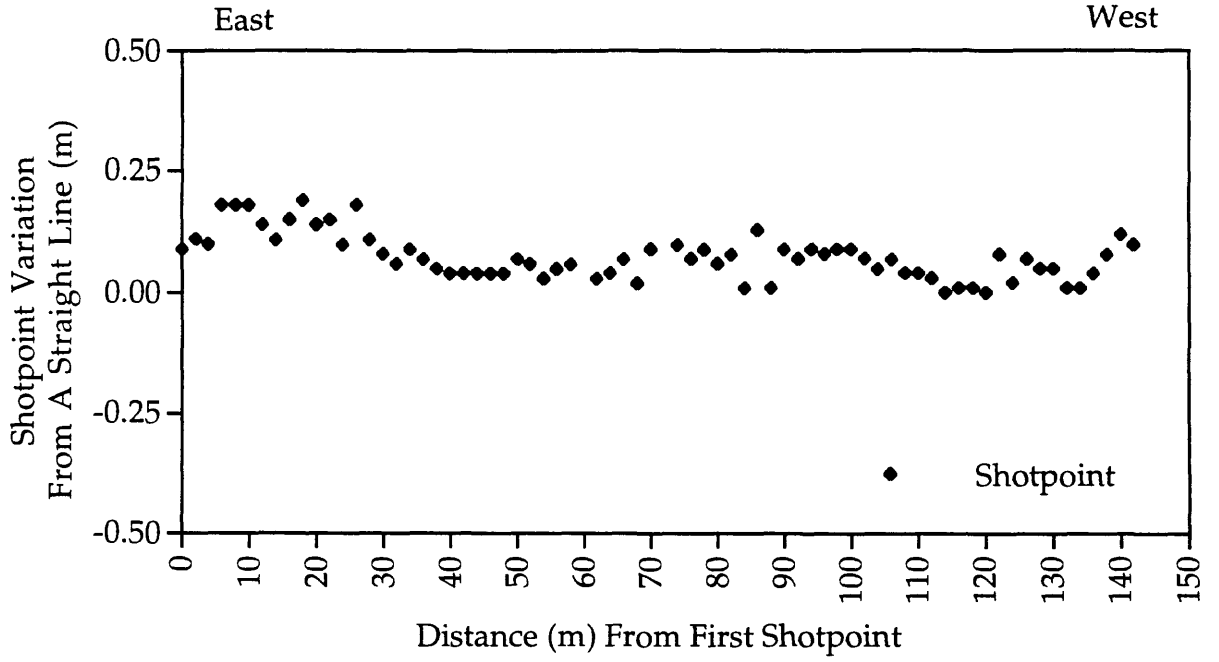

Fig. 3b. Shotpoint variation from a straight line connecting the end points.

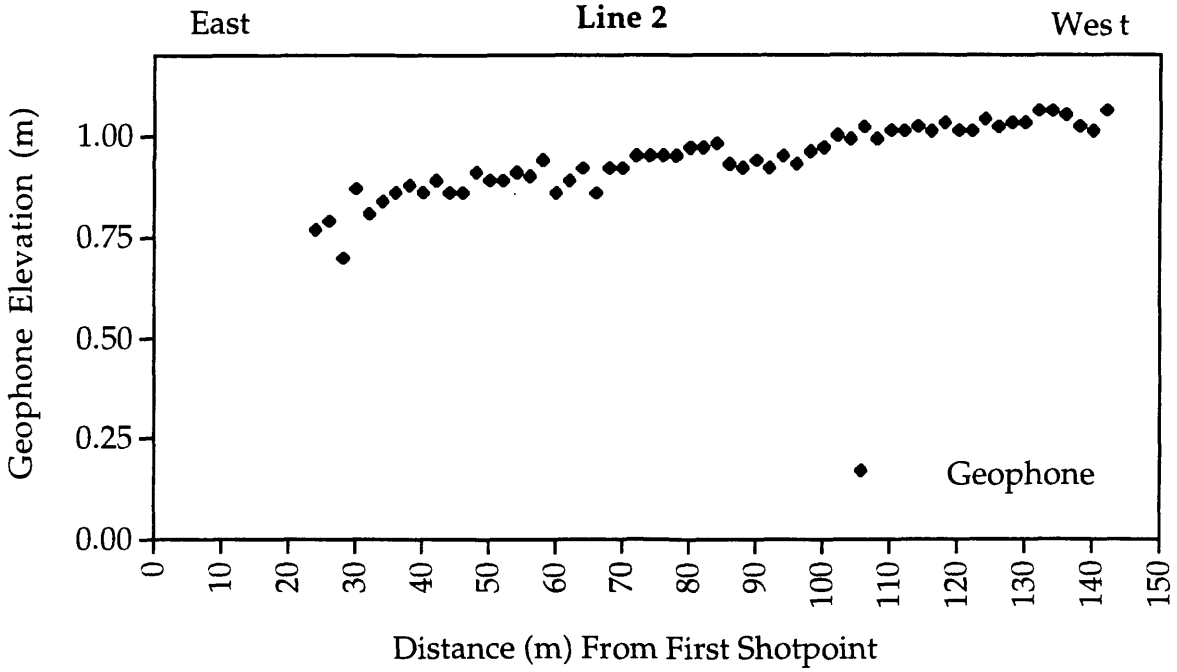

Fig. 4a. Geophone elevations (relative to the topographically lowest geophone along the line) versus distance

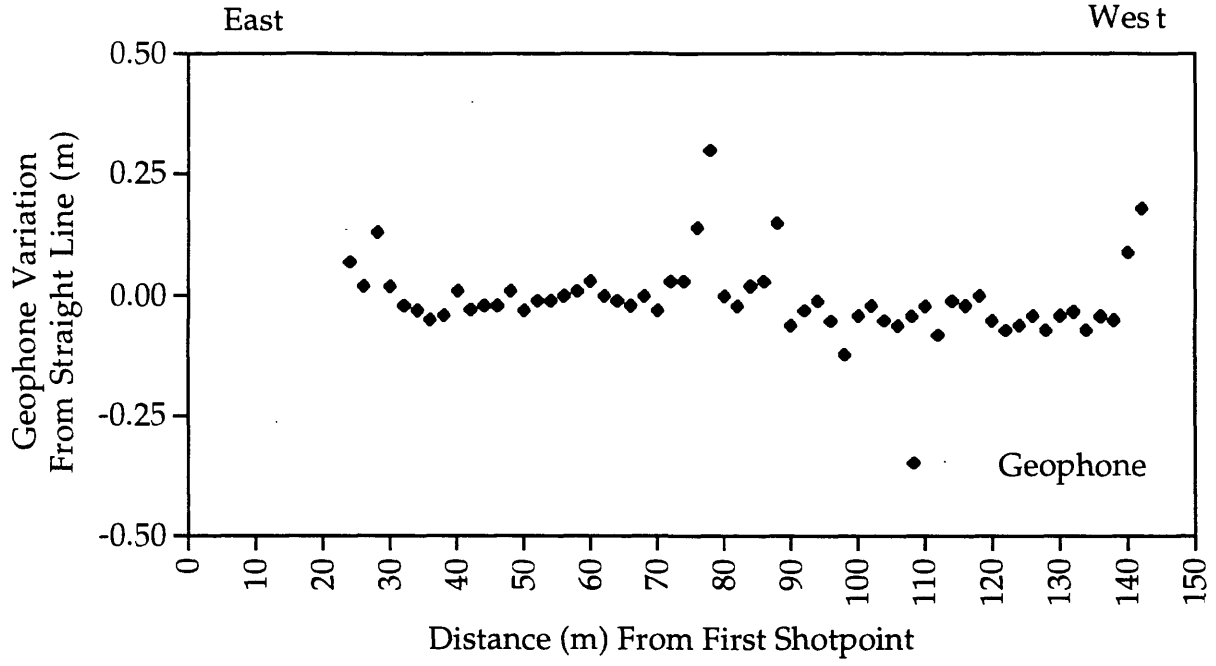

Fig. 4b. Geophone variation from a straight line connecting the end points.

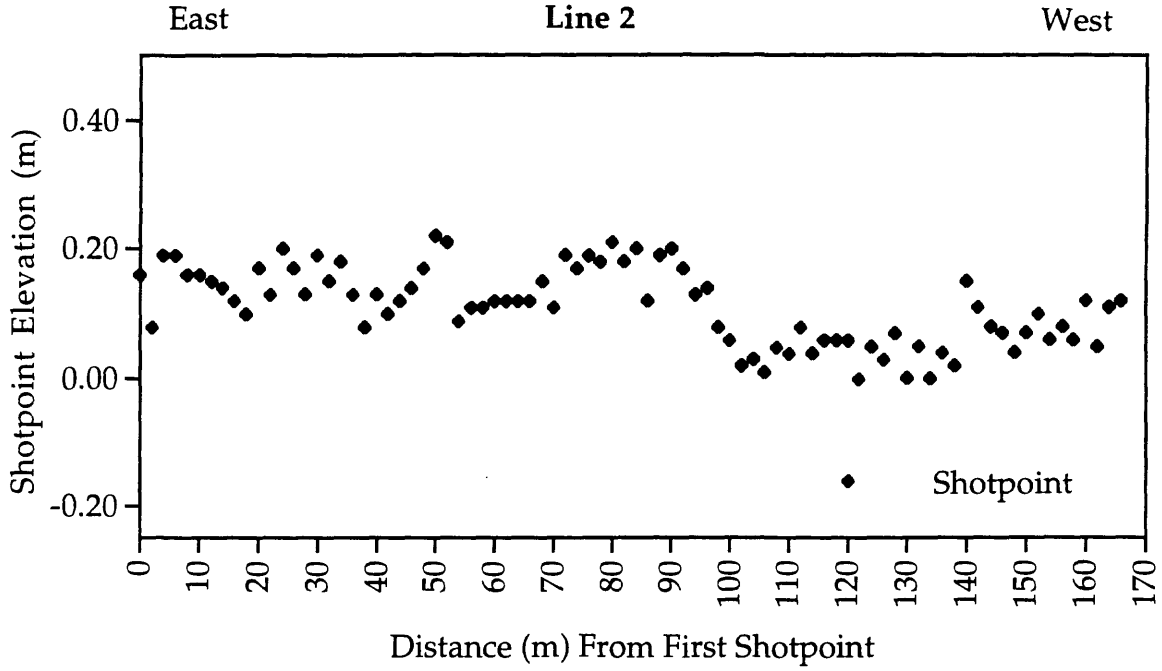

Fig. 5a. Shotpoint elevations (relative to the topographically lowest shotpoint along the line) versus distance.

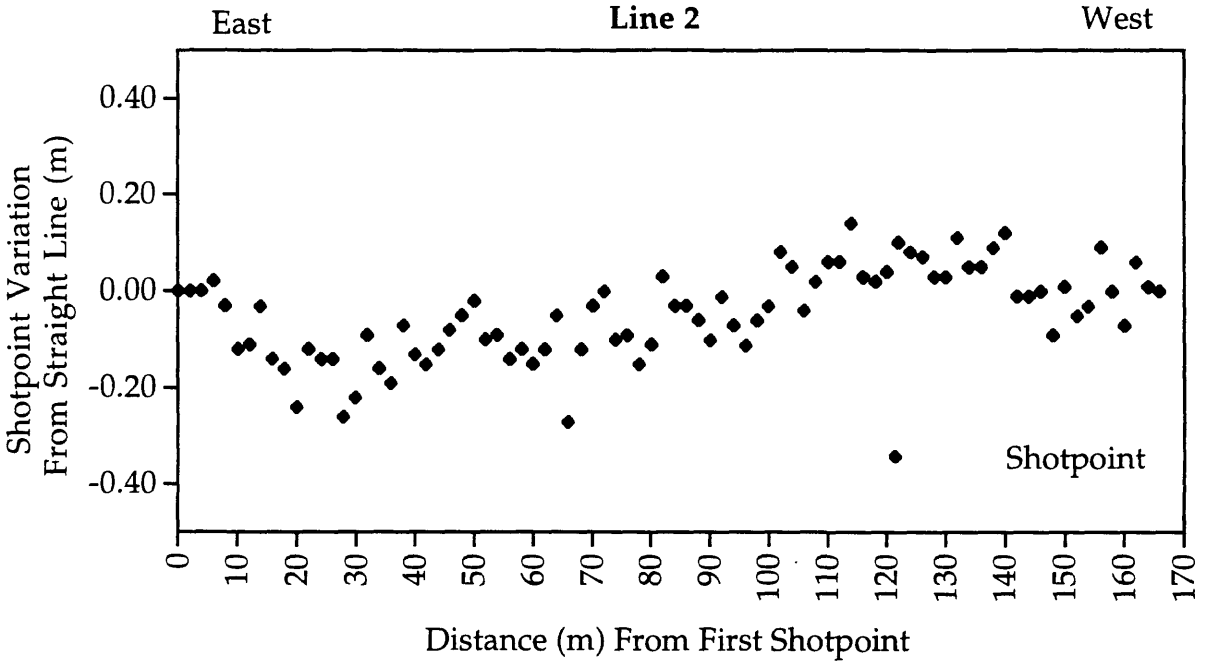

Fig. 5b. Shotpoint variation from a straight line connecting the end points.

The first-arrival data were also processed using seismic refraction techniques using an algorithm developed by Hole (1992) and modified by the authors. The following steps were involved in data processing:

- Geometry Installation
- Trace Editing
- Bandpass Filtering
- Timing Corrections
- Velocity Analysis
- Velocity Inversion
- Moveout Correction
- Elevation Statics
- F-K Filtering
- Muting
- Stacking
- (Migration)

The geometry was installed directly from the electronic distance meters into the Promax processing routine. Bad coupling between geophones and the ground, malfunctioning geophones, and movement or vibrations along or close to the seismic line resulted in unusually noisy traces that were edited. Independent trace editing is employed for each shot gather.

All frequencies below 30 Hz was initially deleted to remove most surface waves, shear waves, and cultural noise. Additional bandpass windows were later utilized to emphasize the shallow subsurface.

In the field, the RX60 seismograph was electronically triggered by the seismic source. Trigger delays between the advent of recording and explosion was generally less than 1.5 ms. Although these were minor timing errors, we also used the uphole times from co-located shots and geophones to correct for the delays.

Initial velocities were determined using several methods. Direct velocities were measured on the shot gathers by measuring both first arrivals and by measuring move out on subsurface reflections. A more robust determination of velocities along the seismic lines was determined by using inversions of the first arrivals. The inversions provided detailed velocities to depths of approximately 30 m. Below 30 m depth, we used the Promax interactive velocity analysis of CDPs and known velocities determined from boreholes. Moveout correction was based on the refraction velocities.

Because there were only minor variations in the elevations along the seismic lines, the elevation statics were minimal. Nevertheless, we applied corrections to elevation variations using the measured velocities and elevation differences.

Simple bandpass filtering did not remove all of the surface waves, air waves, and cultural noises. We used F-K filtering to remove the unwanted arrivals. In cases where F-K filtering did not satisfactorily remove all of the unwanted arrivals and to remove refractions, muting was selectively used.

Both migrated and unmigrated seismic sections were produced; however, because the shallow stratigraphy of interest was largely planar and did not dip significantly, migration did not significantly improve the seismic sections and are not included here.

Seismic Data

Fold

We used a "shoot-through" data acquisition method that resulted in a smoothly varying fold. Minimum folds ranged from about 5 to 10 near the ends the recording array of line 1 and about 10 to 20 near the ends of the recording array of line 2. (Fig. 6). The folds linearly increased to approximate 60 near the middle of the arrays, resulting in more redundancy and deeper imaging near the center of the arrays. Generally, where folds were in excess of about 35, reflections were imaged to depths in excess of 400 m depth (Fig. 7). Areas of low fold near the ends of the arrays, however, imaged progressively shallower reflections.

Line 1 Stacked Seismic Reflection Image

A stacked image of the upper 15 m of the subsurface along line 1 is shown in figure 8. In processing these data, arrivals with velocities between 50 and 250 m/s have been removed with a 1-200-Hz F-K filter, and the data have been bandpassed to emphasize seismic energy between 600 and 1200 Hz. Fourier analysis show that much of the data corresponding to depths above 30 m has appreciable frequency content in excess of 900 Hz. The stratigraphy determined from shallow (~ 5m) wells located along the seismic line are also shown. An extension of the seismic data to depths of approximately 50 m and the stratigraphy from a deep well at Dumbarton Point are shown in figure 9. Both seismic sections show detailed reflectors in the upper 10 m, and the deeper section show reflections from about 25 to 35 m depth.

Line 1 Seismic Velocities

Seismic compressional-wave velocities for the upper 30 m beneath line 1 are shown in figure 10. Velocities range from about 700 m/s near the surface to about 2500 m/s at about 30 m depth. There are minor lateral variations in the velocities of the upper few meters, with lower velocities on the eastern half of the line and at about 130 m. From about 5 to 10 m depth, a low-velocity channel is apparent near the eastern end of the line at about meter 10. At depths below about 15 m there are apparently low velocity channels east of meters 25, at about meter 6, and west of meter 120. Some of these velocity variations may be due to large-scale changes in stratigraphy. We caution, however, that lateral variations in the velocity structure within the 5 m of the end of the array may be due to edge effects unrelated to the velocity structure at the Raychem site.

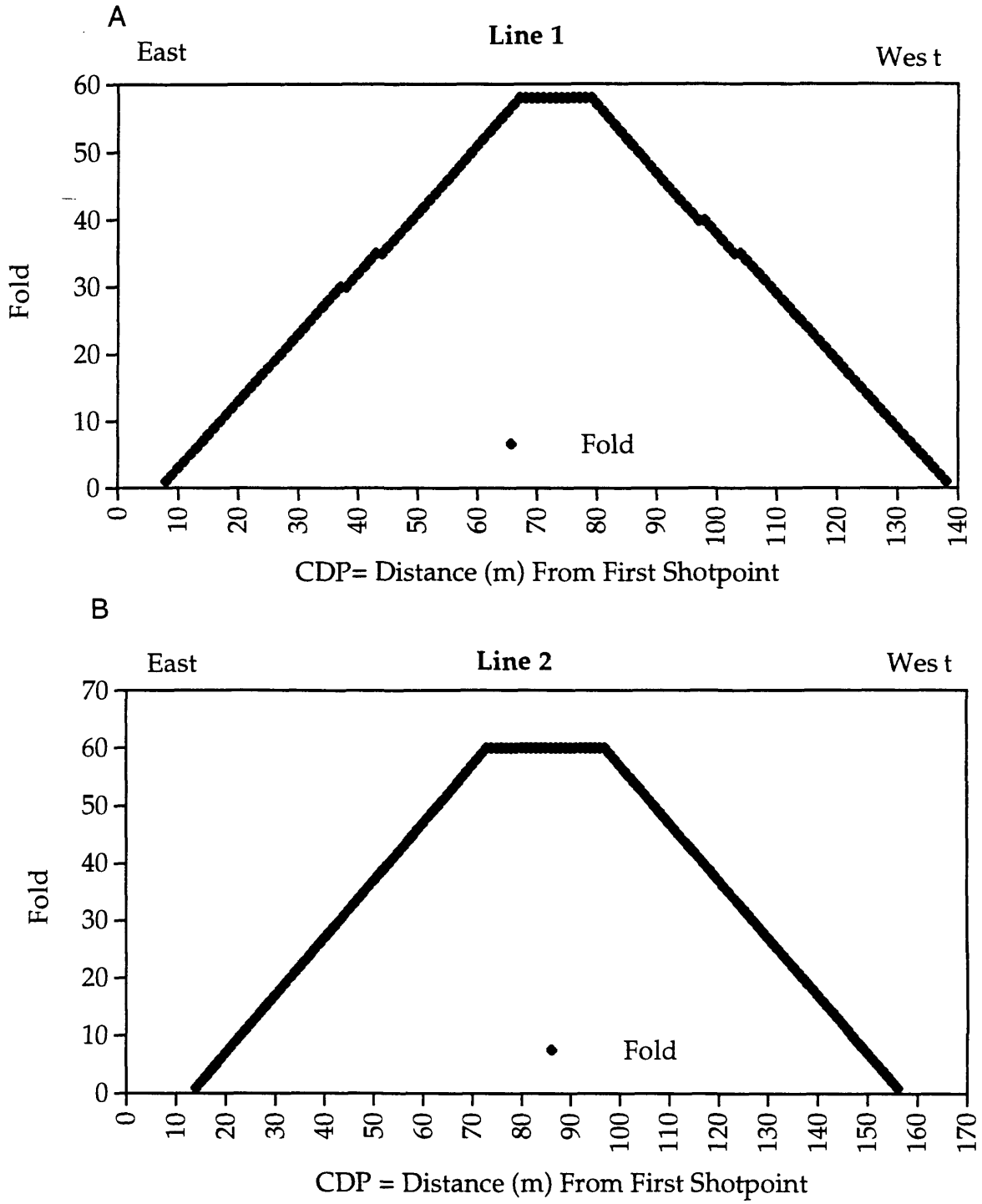

Fig.6 Variation in fold along (a) line 1 and (b) line 2

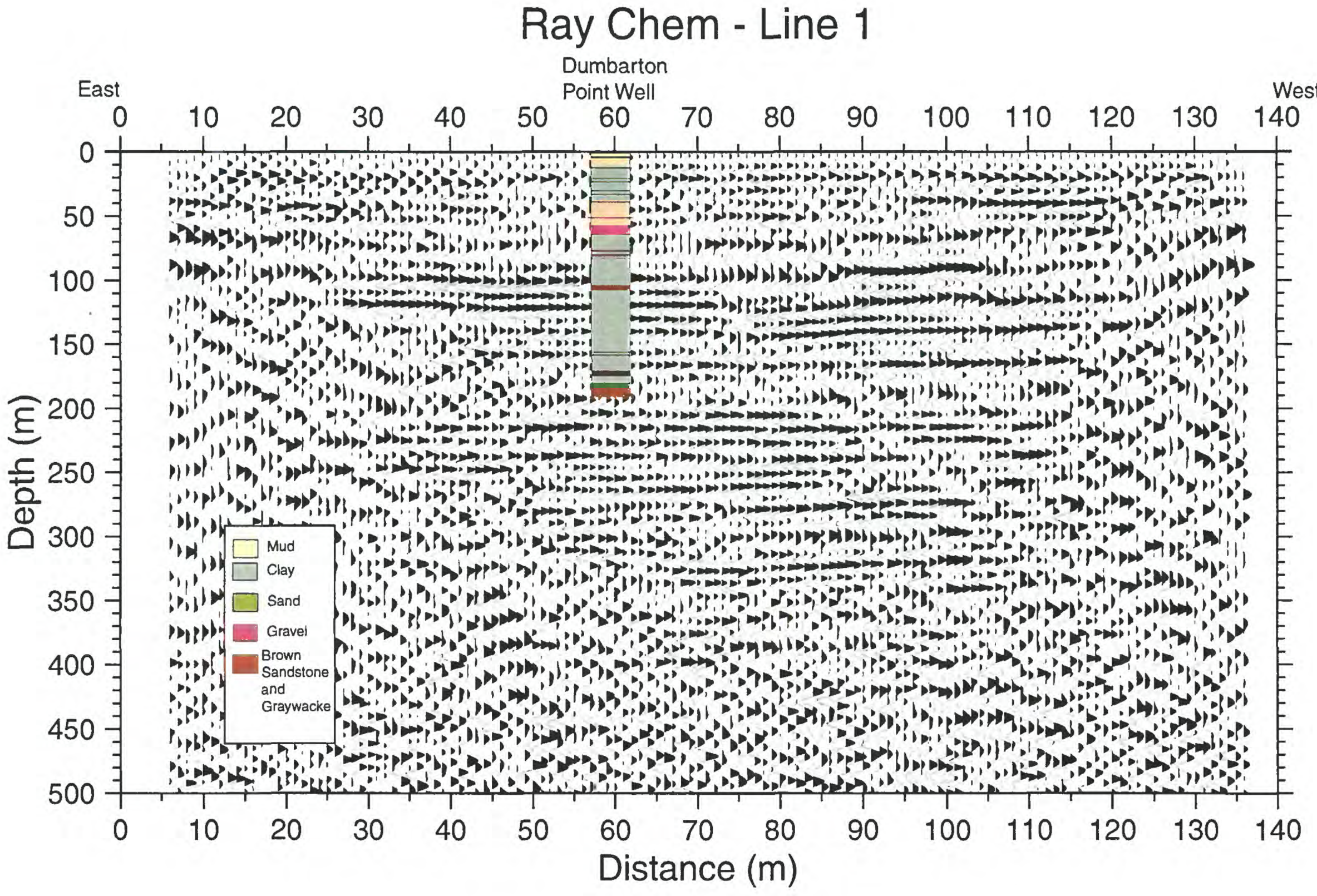

Fig. 7 Stacked seismic section of the upper 500 m beneath line 1. The well log shown is from a well located about 1 km to the east of the Raychem site and described by Warrick (1974). Deeper seismic data are observed only in areas of high fold, near the center of the seismic array.

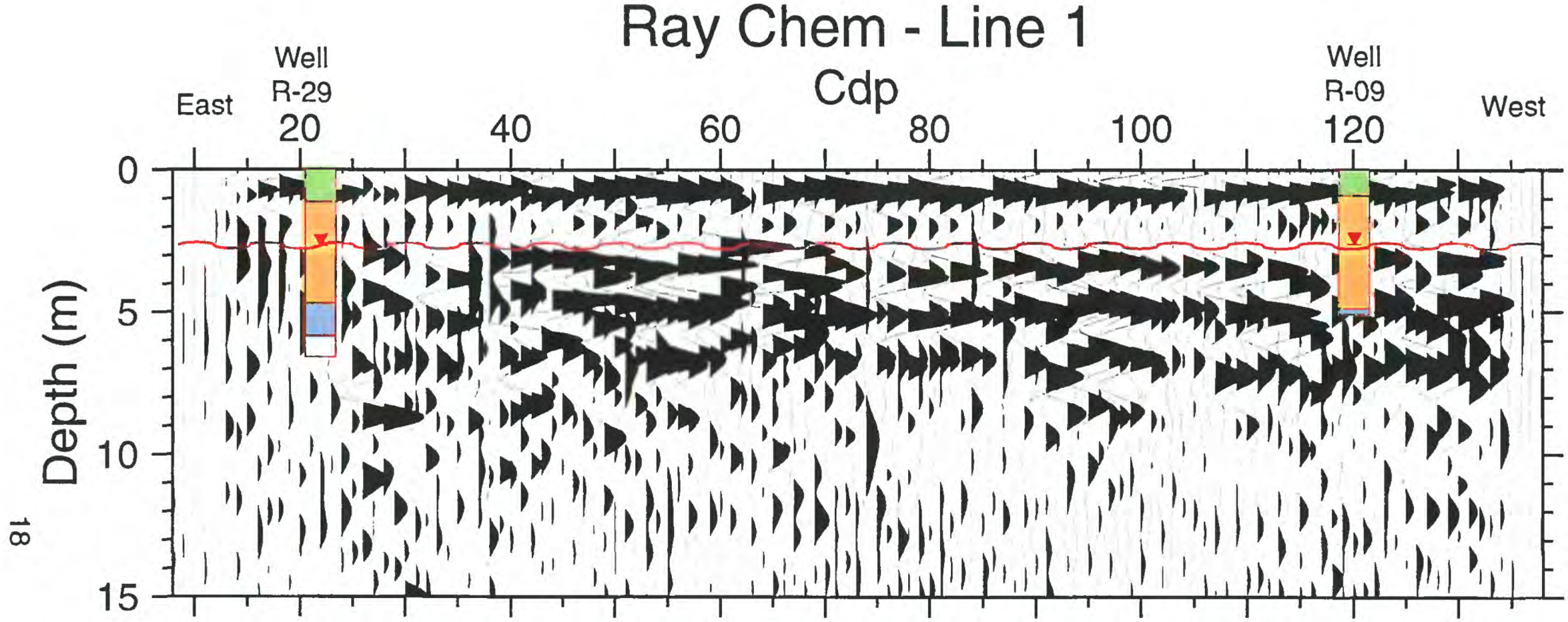

EXPLANATION

- Fill
- Organic clay
- Clayey silt with sand
- Clayey sand
- Water Table

Fig.8 Stacked seismc reflection section of the upper 15 m of Line 1 with well logs for wells located along the seismic line. Well logs were described by Mclaren Consultants. Horizontal axis is in common depth points. Common depth points are approximately 1 m each.

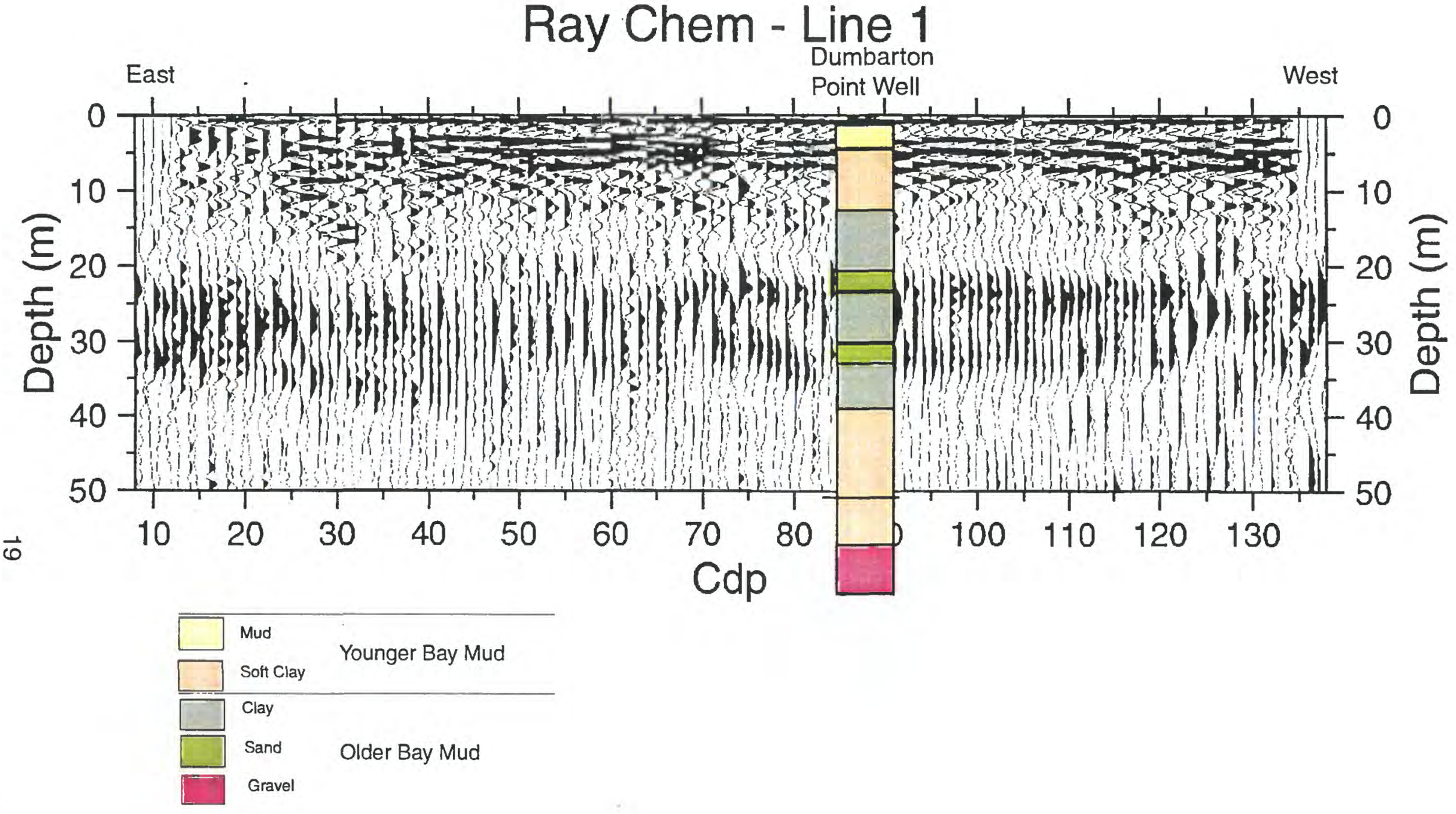

Fig. 9 Stacked seismic reflection section along line 1 with the well log of Warrick (1974). The well was located approximately 1 km to the east of the seismic line. Horizontal axis is in common depth points (CDP). Each CDP is approximately 1 m.

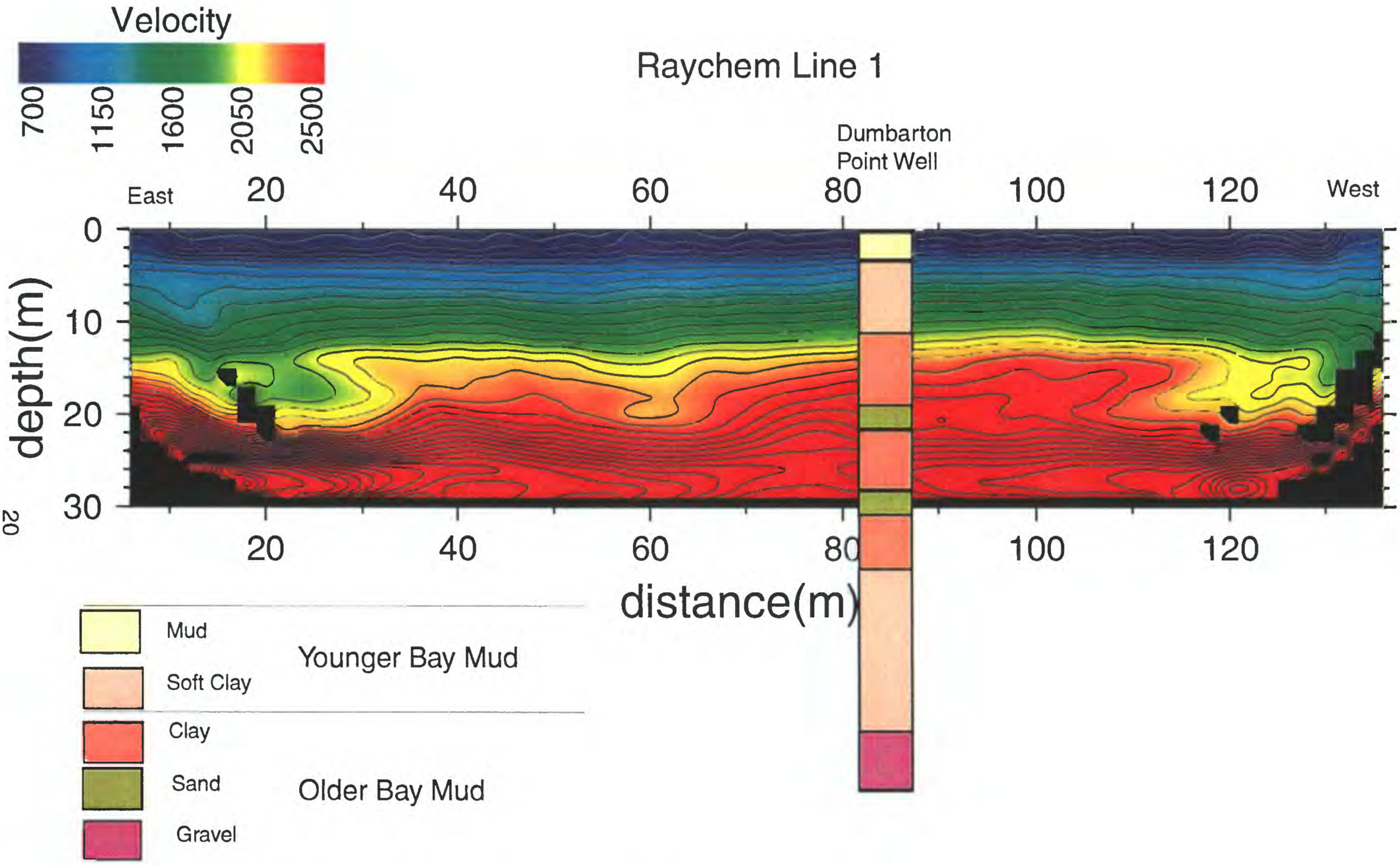

Fig. 10 Seismic velocity inversion for the upper 30 m along line 1. Velocities correlate with differences among mud, clay, and sand. The well shown is from a borehole approximately 1 km east of the seismic profile (Warrick, 1974).

Line 2 Stacked Seismic Reflection Image

A stacked seismic reflection image of the upper 15 m beneath line 2 and the stratigraphy determined from nearby shallow (< 5 m) wells are shown in figure 11. Due to datum differences, some of the reflections observed along line 1 are not present in the upper 2 m of line 2. The seismic data shown have the same processing scheme applied as that of line 1. An extension of the line 2 seismic reflection data to 100 m and the stratigraphy from a borehole at Dumbarton Point (Warrick, 1974) are shown in figure 12. The deeper seismic section shows reflections from about 25 to 50 m depth on the eastern end of the profile, dipping westward. As observed along line 1, the section between about 20 and 40 m depth near the eastern end of the profile is highly reflective, but unlike along line 1, individual reflectors are clearer, perhaps to greater frequency retention along line 2. The higher frequencies at depths in excess of 20 m suggests that the attenuation characteristics of the layers between about 5 and 20 m differ appreciably between lines 1 and 2. Along both lines 1 and 2, however, the subsurface stratigraphy from about 3 m below the surface to depth of approximately 20 m is similar, with few reflectors in that depth range.

Line 2 Seismic Velocities

Compressional-wave seismic velocities beneath line 2 range from about 700 m/s at the surface to about 2100 m/s at 20 m depth (Fig. 13). As observed along line 1, velocities are lower along the eastern part of the line for depths above about 5 m, except for tow localized low-velocity areas at about meters 120 to 130 . Velocities above 5 m depth are highly variable within the first few meters of the subsurface, varying by as much as 400 m/s laterally. From about 5 m to about 15 m depth, lower velocities are concentrated in the distance range from about meters 20 to 40 and meters 120 to 140, where velocities vary laterally by as much as 700 m/s.

Interpretative Sections

We suggest that reflections within the upper 50 m beneath line 1 originate from a combination of lithologic and physical boundaries (Table 1). By combining the information from the stacked sections with that from the velocity inversions and existing boreholes, we present an interpretative cross section along both lines (Figs. 14 and 15). Along line 1, the seismic stratigraphy within the upper 6 m was correlated with the stratigraphy determined from wells R-09 and R-29, and the seismic stratigraphy from line 2 was correlated with that determined from wells R-28 and R-31. For the deeper sections, we use lithologic information from nearby wells at Dumbarton Point (Warrick, 1974). Within the upper 25 to 30 m, the velocity data acquired during this survey are useful in differentiating between the thicker sand-gravel and clay units because the clays are generally higher in velocity.

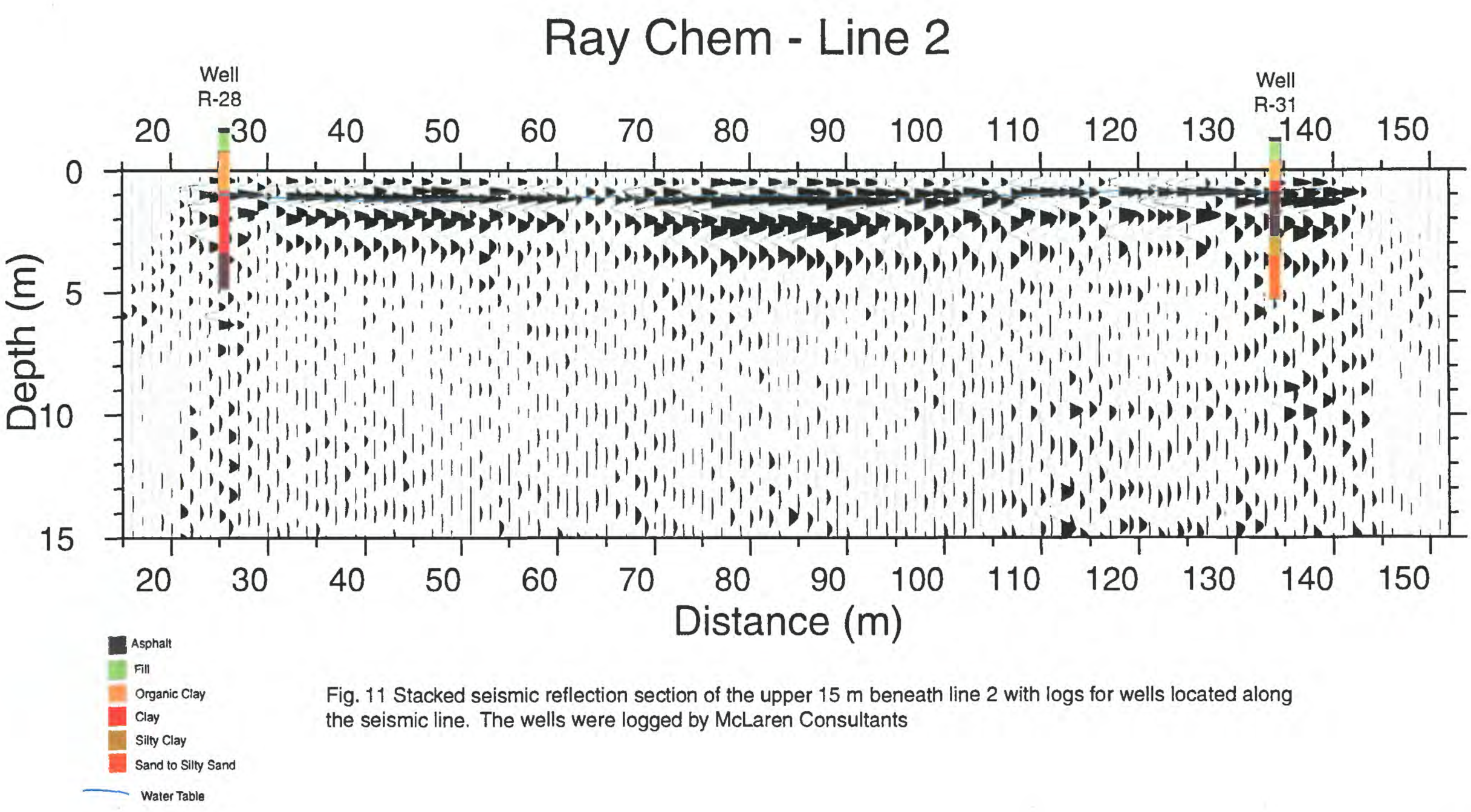

Fig. 11 Stacked seismic reflection section of the upper 15 m beneath line 2 with logs for wells located along the seismic line. The wells were logged by McLaren Consultants

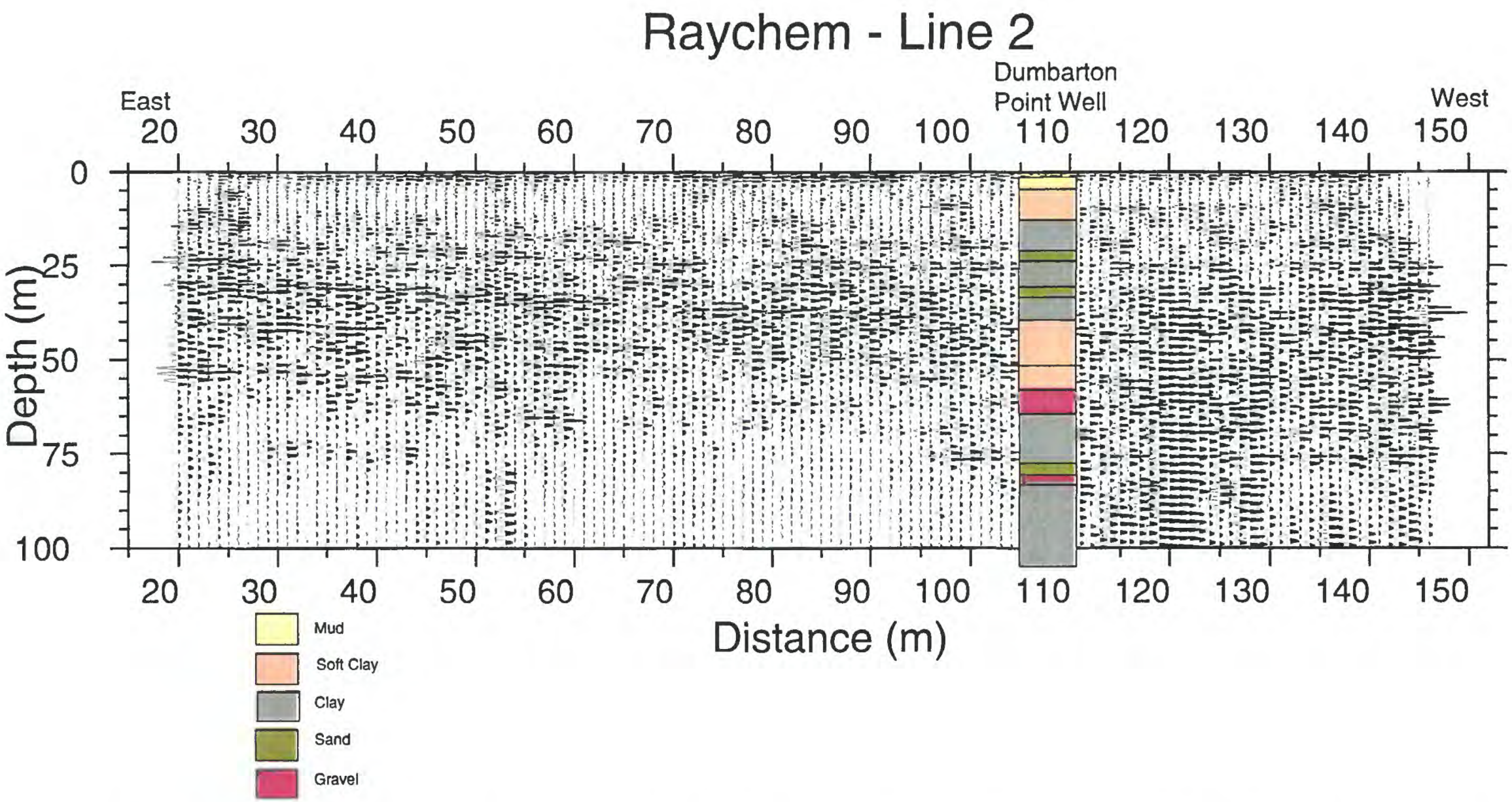

Fig. 12 Stacked seismic reflection section along line 2 with a simplified well log from Warrick (1974). The well was located approximately 1 km east of the seismic line.

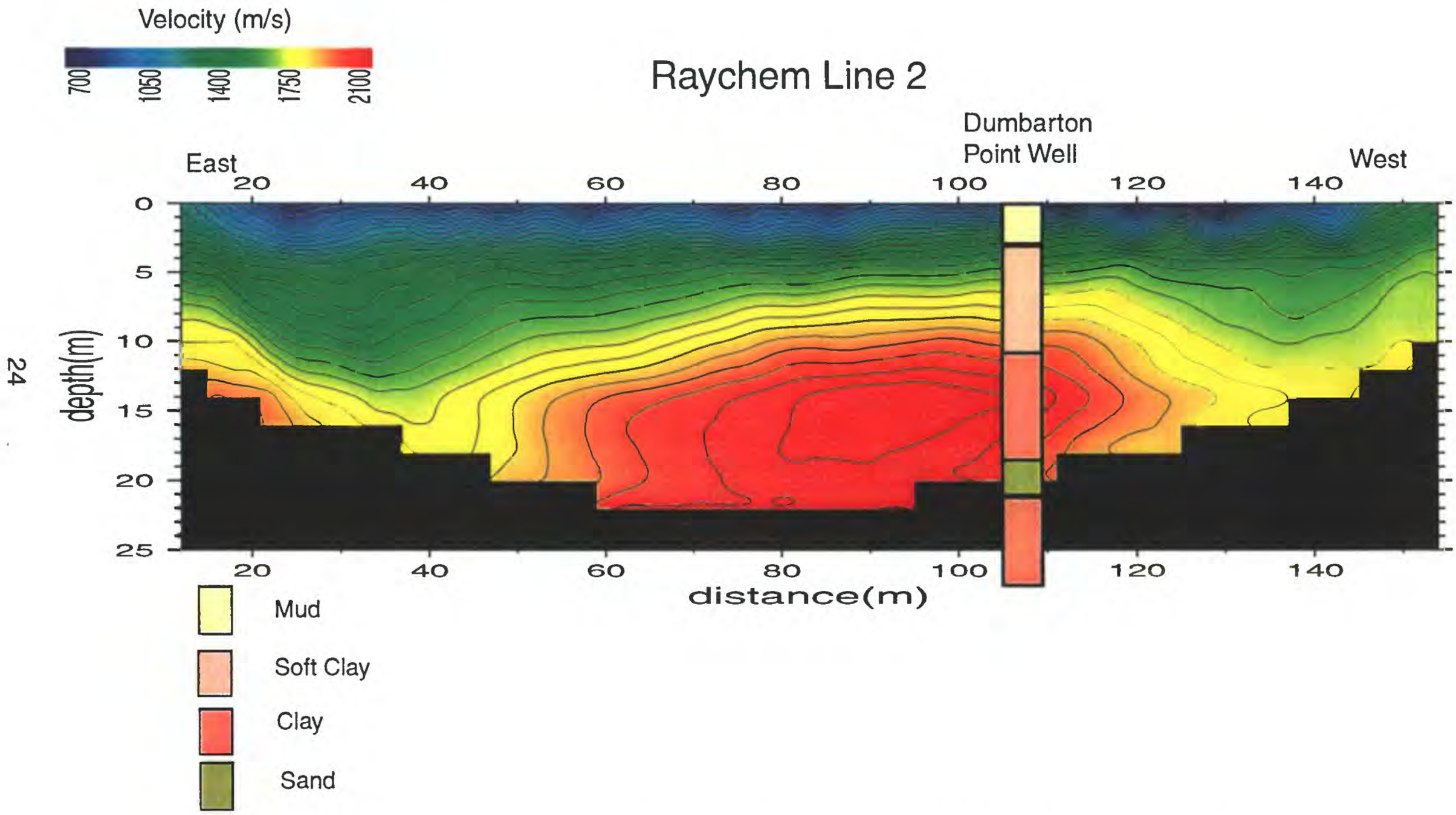

Fig. 13 Seismic velocity inversion for the upper 25 m along line 2 at the Raychem site. The well shown is from a borehole located approximately 1 km east of the seismic line (Warrick, 1974).

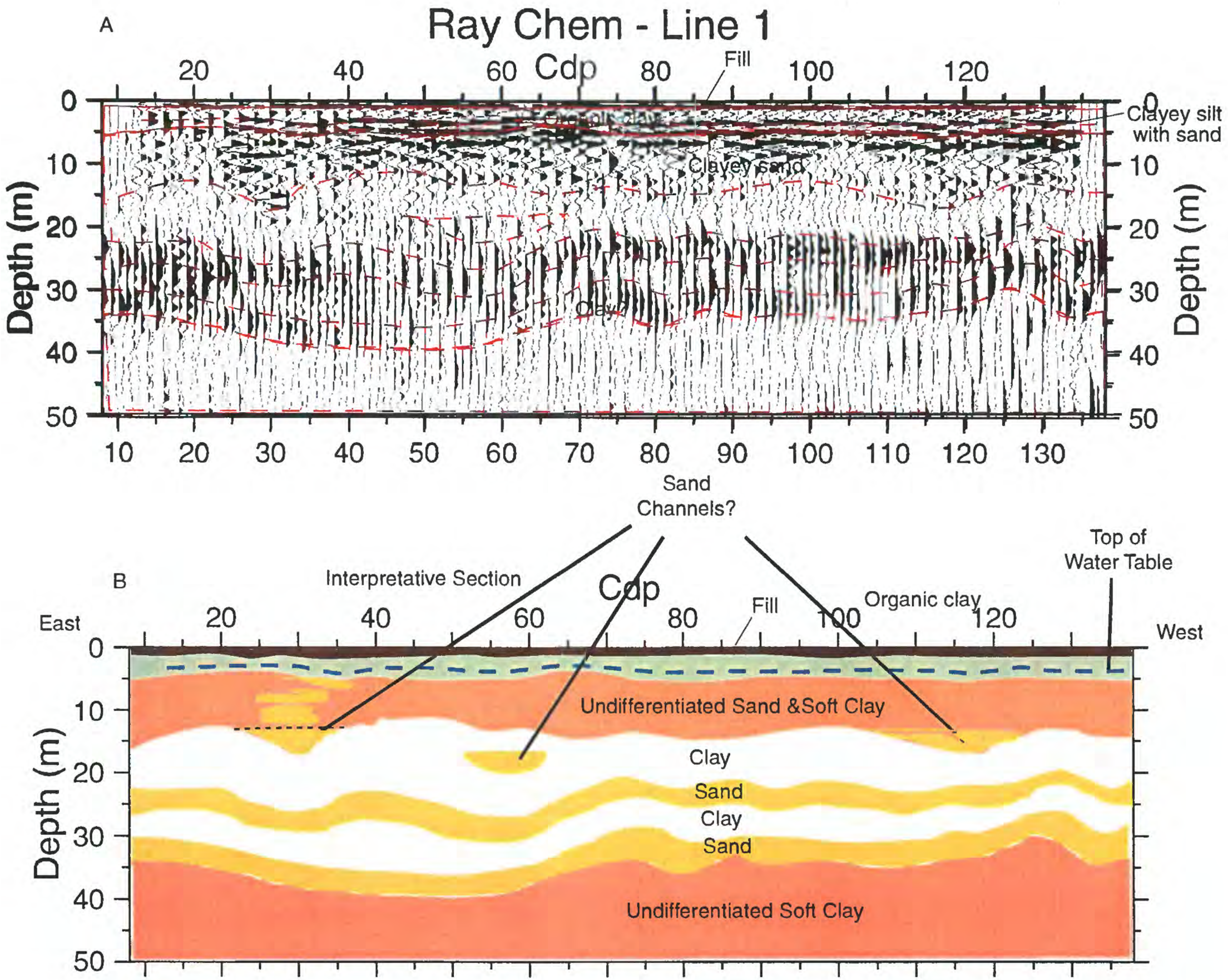

Fig. 14 (a) Seismic data with reflectors outlined. (b) Interpretative section based on borehole and seismic data.

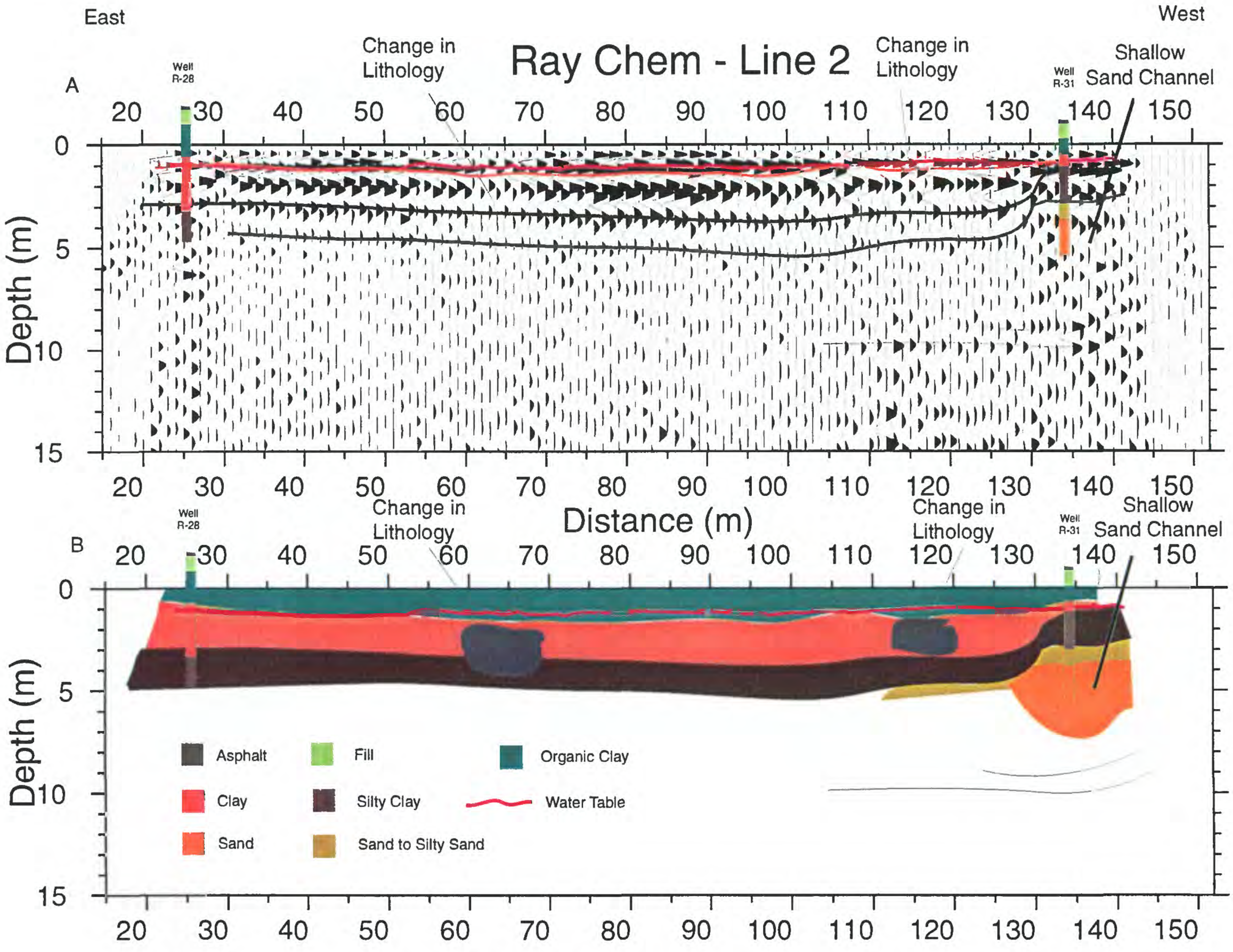

Fig. 15. (a) Seismic section for upper 15 m of line 2 with interpreted lateral variation in stratigraphy. (b) Interpretative geologic cross section.

Line 1 Interpretation

On the basis of the seismic velocity data, the seismic reflection data, and existing borehole data, we provide a summary interpretation of the stratigraphy beneath line 1 in figure 14.

The first reflection on the seismic section corresponds to the interface between man-made fill material and an underlying organic clay located at approximately 1 m beneath the ground surface. The reflection from this layer occurs at the same depth in both the borehole (Table 3) and the seismic section (Fig. 13). The contact between the fill, consisting largely of compacted gravel, and the clay varies in depth by less than 1 m along the length of the profile. The velocity model shows that the surface fill generally has velocities less than about 800 m/s, but the velocities rapidly increase within the clay layer from about 700 m/s at about 1 m depth to about 1200 m/s at the depth of the water table (3 m depth) (Fig. 10).

The second prominent reflection on the seismic section corresponds to the top of the water table, located at about 3 m depth. The water table occurs within the organic clay layer (Fig 13), and has corresponding velocities of approximately 1200 m/s. The water table appears to vary more in elevation along the profile than does the clay-fill contact, but the water table appears to vary less than 1.5 m in depth. At about CDP 30, reflections from the water table and the underlying layers appear to be scattered, suggesting some structural complexity. On migrated sections, the layer appears to be convex in shape, suggesting an incision into the clay layer.

Two reflections from additional layers (Clayey silt with sand and clayey sand) occur at about 5 and 6 m below the surface, as determined from the borehole (Fig. 9). These layers can be traced along the length of the seismic profile, but perhaps due to the structural complexity near CDP 30, the reflections are more difficult to follow on the eastern end of the profile. The reflections from the 5- and 6-m-deep layers vary in amplitude and depth, but are generally consistent with the borehole logs at the locations of the boreholes.

At approximately 20 m to 25 m depth, there is a 15- to 20-m-thick series of reflectors extending across the length of the profile. Correlations with 180-m-deep borehole data from about 1 km to the east shows that there are two ~10-m thick layers of clay separated by thin sand layers in the depth range from about 20 m to about 40 m. Compressional-wave velocities increase to more than 2500 m/s at this depth, and the velocity gradients significantly increase. Both of these velocity characteristics are consistent with a dominantly clay composition. At about 50 to 60 m distance and 20 m depth, the reflection data show structural complexities that are consistent with incisions or sand channels in the clay. The velocity data also show similar indications at this depth and distance, as well as indications of possible channels at about 20 m and 120 m distance.

Line 2 Interpretation

Line 2 was located within a drainage, approximately 2 m below the elevation of the Raychem property. The seismic velocities along line 2 vary from about 700 m/s to more than 1000 m/s at the surface and likely results from lateral variations in water and organic content at the surface. Although line 2 was located adjacent to two wells, the seismic data cannot be directly correlated with the borehole stratigraphy because of the elevation difference. The borehole statigraphy can be approximately correlated with the seismic data by removing the first 1.5 m of the borehole stratigraphy (Table 4).

Well R-31

At least 4 reflections extend across the seismic section, but the strength of the reflectors vary appreciably with distance (Fig. 16). If the first 1.5 meters of the borehole stratigraphy are removed, then the first reflector at about 0.5 m corresponds to a reflection from the interface between the first clay layer and an underlying silty clay. The second and most continuous reflector at about 1 m depth corresponds to the water table. The third reflector at about 2 m depth appears to be discontinuous but produces strong amplitude reflections over most of the seismic line. This reflector corresponds to the interface between a silty clay and a sandy layer. The fourth reflector at about 3.5 m depth does not produce strong reflections, and we are uncertain of its location near well R-31. However, weak reflections between 3 and 4 m depth may result from the interface between a "sand to silty sand" and a "sand", as described on the well logs. A slight westerly dip is inferred by the seismic data.

Well R-28

The sequence of reflectors change across the seismic line, but the most prominent reflector, the water table, is continuous (Fig. 16). In well R-28, the water table is located at approximately 2.5 m depth (Table 4). After adjusting for the topographic difference between the surface at the borehole and that at the seismic profile, a prominent, continuous reflection can be correlated with the water table at about 1 m beneath the surface. A minor reflection just above that of the water table correlates with the depth to the bottom of an organic clay. Because this organic clay is underlain by another clay (with ~10% gravel), the impedance contrast between the two layers is probably not particularly high. Therefore, we expect the reflection to be weak at the interface between the two clays. We also observe a strong reflection at about 2 m beneath the surface, but there is no lithologic contrast listed in the borehole log that corresponds to the depth of this reflection. A weak reflection at about 3 m below the surface correlates with the interface between two clays, a greenish clay with 10% gravel content and a silty clay with increasing fine sand with depth and 10% gravel. Because these two layers are described similarly, we would not expect a strong reflection from the interface between the two layers.

Table 3 Stratigraphy determined from wells R-29 and R-09, adjacent to line 1 (from Harza Consulting Engineers).

R-29

Depth Range	Stratigraphy	Description
0-1.2 m	Gravel	Man-made fill
1.2m-5.0 m	Organic Clay	10% caliche & gravel
2.75 m	*Water Table*	*Static level; 3/13/95*
5.0 m - 6.0 m	Clayey Silt/Sand	80% fines; 20% Sand
6.0 to Bottom	Clayey Sand	~8% gravel; 39% fines

R-09

Depth Range	Stratigraphy	Description
0-1 m	Gravel	Man-made fill
1 m-5.0 m	Organic Clay	10% caliche & gravel
2.75 m	*Water Table*	*Static level; 3/13/95*
5.0 m -5.5 m	Clayey Silt/Sand	80% fines; 20% Sand

In the 20 to 50-m depth range, a number of discrete reflectors with westerly dips are implied by the seismic reflection data. One of the most prominent reflectors at depths of about 35 m appears to be discontinuous or incised at about 65 m distance range, as implied on line 1. In the shallower subsurface (<25 m), a discontinuous reflector at about 20 m depth (and at 40 m and 120 m distance) correlates with velocity anomalies at those locations.

Table 4 Stratigraphy determined from wells R-31 and R-28 along line 2. (from Harza Consulting Engineers)

R-31

Depth Range	Stratigraphy	Description
0-0.15m	Asphalt	Pavement
0.15-0.9 m	Fill	Gravel
0.9-1.8 m	Organic Clay	80% fines; 20% organic
1.8-2.3	Clay	90% fines; 5% sand; 5% gravel
2.2 *m*	*Water Table*	*Static level; 2/6/95*
2.3-4.1 m	Silty Clay	70% fines; 20% Gravel; 10% sand
4.1-5.0 m	Sand, Silty Sand	81% fines, 19% gravel
5.0-6.5 m	Sand	86% fine-coarse sand; 8% gravel, 5% fines

R-28

Depth Range	Stratigraphy	Description
0-0.15 m	Asphalt	Pavement
0.15-0.9 m	Fill	Gravel
0.9-2.45 m	Organic Clay	80% fines; 20% organic
2.6 *m*	*Water Table*	*Static level; 2/7/95*
2.45-5.0 m	Clay	90% fines, 10% caliche/gravel
5.0-6.5 m	Silty Clay	80% fines; 10% Gravel; 10% caliche

It is difficult to correlate individual reflections from the seismic sections with the borehole data that is 1 km to the east at Dumbarton Point (Warrick, 1974), but the general sequence of a series of reflectors at about 20 m to about 75 m depth is consistent with a series of sand, gravel, and clay layers found in the borehole (Table 1).

Correlations Between the Two Lines

Lines 1 and 2 differed in elevation because line 1 was located on man-made fill within the Raychem property, and line 2 was located within a lower-lying drainage adjacent to the Raychem property (Fig. 1b). Therefore, reflections imaged in the upper ~2 m beneath line 1 will not be present on line 2. Reflections from the water table and the base of the organic clay can, however, be correlated along both lines. Reflections from individual clay layers that differ only slightly lithologically are more difficult to correlate across the two lines without a seismic profile that connects the two lines. Areas with probable sand channels incised into the clay aquitards can be seen on both seismic profiles at both shallow and deeper depths, but these probable sand channels are not linear features that occur at the same longitude on both lines. On line 1, a shallow (< 10 m) channel is implied by the low velocities and discontinuous reflections at about 15 m from the eastern end of the line, but on line 2, the shallow channels are implied at 110-140 m from the eastern end. Deeper channels (10 to 20 m) on line 1 are inferred at about 20, 60, and possibly 120 m distance on line 1. On line 2, deeper (<25 m) discontinuous reflections may correspond to sand layers at several locations, including about meters 35-40 m and meters 120-140 m.

Correlations Between Borehole Velocities and Imaged Velocities

Warrick (1974) measured velocities in the boreholes at Dumbarton Point at three different depths, 12 m, 40 m, and 185 m using a laterally moving surface sources and sensors placed in the boreholes at those depths. These depths were chosen so that velocities could be measured in the younger bay mud (to 12 m), the older bay sediments (to 180 m), and in the Franciscian bedrock (185 m). Warrick (1974) measured P-wave velocities of 1360 m/s for the younger bay muds and 1740 m/s to 1840 m/s for the older bay sediments. The velocities that we measure at those depths differ appreciably from those of Warrick (1974). For example, we measure velocities of approximately 1700 to 1900 m/s at 12 m depth and velocities of approximately 2500 m/s at depths as shallow as 30 m.

The difference in velocities are largely a function of how the two data sets were acquired. By placing sensors at select depths, Warrick (1974) effective averaged the velocities between the surface and those at the depths of the sensor. By placing the sensors at the surface over laterally extensive array, we were able to measure progressively deeper velocities with offset.

Because the shallow velocities were determined at each point along our seismic array, the deeper velocities could be calculated.

We found that velocities ranged from about 700 m/s to about 2000 m/s in the upper 12 meters. If we take a simple average of those velocities at even intervals (700 m/s at the surface, 1400 m/s at 6 m, and 2000 m/s at 12 m), we obtain an average velocity of about 1366 m/s, similar to the velocity measured by Warrick (1974). At 30 m depth, we measured a velocity of about 2500 m/s compared to an average velocity of 1740 to 1840 m/s measured by Warrick at 40 m depth. However, if we use a simple average as above (700 m/s at the surface, 1400 m/s at 6 m, 2000 m/s at 12 m, 2200 m/s at 18 km, 2400 m/s at 24 m, and 2500 m/s at 30 m), we obtain an average velocity of about 1880 m/s, only slightly higher than that obtained by Warrick at 40 m depth. According to the well log on figure 10 sand layers and softer clays are also present below 30 m depth. The sand and softer clay would be representative of significantly lower velocities than 2500 m/s, thus the overall average velocity to 40 m depth would be slightly lower than our average to 30 m. Because of averaging caused by borehole velocity measurement techniques, assumed near-surface velocities can vary by as much as about 50% and as much as 30%. Although these measurements are for compressional-wave velocities, it is likely that the shear-wave velocities differ in a similar way.

Summary and Conclusions

The stratigraphic sequence at the Raychem site in Menlo Park, California, as revealed in boreholes, can be laterally mapped using a combination of high-resolution seismic reflection and refraction imaging techniques. Although there are lateral variations in stratigraphy, correlations among velocities and reflectors with borehole-determined stratigraphy from distant wells suggest that the overall stratigraphy from the surface to basement rocks is somewhat continuous at the bay margin. This correlation suggests that high-resolution seismic imaging can be used to characterize the stratigraphy and velocity structure for purposed of environmental and earthquake hazards assessment.

At the Raychem site, we interpret several sand channels incised into the clay aquitard layers at shallow (<10 m) depth and at deeper (20-25 m) depths. The geographical locations of these apparent sand channels vary considerably over distances of at least 120 m. Several seismic profiles acquired over the site could be used map the subsurface lateral variation in the sand channels. because the sand layers are represented by lower velocities and are represented by less coherent reflections.

Accurate characterization of the velocity structure at the San Francisco Bay margin is important because numerous high-occupancy buildings and industrial complexes are built there. Because there are few velocity measurements and little is known of the structural variations in the subsurface, detailed velocity measurements of the type presented in this survey are needed. In modeling strong ground motions from future

earthquakes, the calculations differ appreciably depending on the velocities assumed for the bay muds and older bay sediments. Our measured refraction velocities at any given depth differ by up to 50% from the average velocities determined in borehole measurements; yet, our velocities are similar to those measured in boreholes when averaged with depth. This discrepancy in averaged and actual velocities demonstrates that care must be taken in applying velocities determined from borehole measurements when developing numerical models of ground shaking.

Data Availability

The digital seismic data for this investigation are available in SEG-Y format on 8 mm tapes. The data are available as shot gathers that have been corrected for elevation and timing differences or as stacked sections. For a copy of these data, please contact the Principal Investigators at:
U. S. Geological Survey, Earthquake Hazards Team, 345 Middlefield Rd. MS 977, Menlo Park, California 94025

Acknowledgments

This investigation was undertaken at the request of Peter Martin and Christopher Farrar of the U. S. Geological Survey Water Resources Division. We thank Tom Rooze for field assistance and permissions. Field assistance was provided by Katherine Favret, Monique Jaasma, Janice Murphy, August Nelson, and Jeroen Preiss. We thank John Hamilton for electronic surveying and Tanni Abramovitz for reviews.

References

Borcherdt, R. D.,1970, Effects of local geology on ground motion near San Francisco Bay: Seismol. Soc. Am Bull., v. 60, p. 901-904

Borcherdt, R. D., J. F. Gibbs, and K. R. Lajoie, 1975, Prediction of maximum earthquake intensity in the San Francisco Bay region, California, for large earthquakes on the San Andreas and Hayward faults: U. S. Geol. Surv. Misc. Field Studies Map, MF-709, 11 p.

Borcherdt, R. D., and G. M. Glassmoyer, 1990, On the characteristics of local geology and their influence on strong ground motion generated by the Loma Prieta earthquake in the San Francisco Bay region, California: Seismological Society of America Bulletin, v. 82, p. 603-641

Hole, J. A., 1992, Nonlinear high-resolution three-dimensional seismic travel time tomography, J. Geophys. Res., v. 97, p. 6553-6562

Warrick, R. E., 1974, Seismic Investigation of a San Francisco Bay mud site, Bull Seismol. Soc. Am, v. 64, pp. 375-385

Distances and elevations along seismic line Ray Chem 1.
Measurements are relative to first shotpoint.

Shot Number	Shot Dist. (m)	Shot Elev. (m)	Receiver Dist. (m)	Receiver Elev. (m)
1	0	0.09		
2	1.97	0.11		
3	3.89	0.1		
4	5.86	0.18		
5	7.96	0.18		
6	9.89	0.18		
7	11.92	0.14	11.9	0.1
8	13.92	0.11	13.86	0.06
9	15.93	0.15	15.93	0.07
10	17.94	0.19	17.9	0.1
11	19.94	0.14	19.91	0.1
12	21.96	0.15	22	0.08
13	23.88	0.1	24.02	0.12
14	25.96	0.18	25.99	0.17
15	27.91	0.11	28	0.08
16	29.9	0.08	30	0.06
17	31.93	0.06	31.98	0.05
18	33.91	0.09	33.98	0.09
19	35.95	0.07	36.01	0.08
20	37.91	0.05	37.99	0.06
21	39.86	0.04	40	0.06
22	41.95	0.04	41.99	0.06
23	43.92	0.04	43.98	0.07
24	45.96	0.04	45.76	0.06
25	47.94	0.04	48.01	0.03
26	49.94	0.07	49.98	0.05
27	51.91	0.06	51.98	0.05
28	53.9	0.03	54	0.02
29	55.89	0.05	55.99	0.05
30	58	0.06	57.98	0.03
32	61.87	0.03	59.98	0.04
33	63.91	0.04	61.96	0.05
34	65.98	0.07	63.97	0.06
35	67.97	0.02	65.99	0.07
36	69.97	0.09	67.98	0.05
38	73.95	0.1	69.98	0.02
39	76.01	0.07	71.99	0.02
40	77.97	0.09	73.98	0.03
41	79.99	0.06	75.98	0.05
42	82.03	0.08	77.98	0.07
43	83.99	0.01	79.95	0.04
44	85.99	0.13	81.97	0.08

45	88	0.01	83.96	0.08
46	89.93	0.09	85.97	0.09
47	92.07	0.07	87.95	0.07
48	94.03	0.09	89.95	0.08
49	95.97	0.08	91.97	0.04
50	97.85	0.09	93.96	0.04
51	99.9	0.09	95.96	0.04
52	101.94	0.07	97.96	0.03
53	103.91	0.05	99.96	0.03
54	105.97	0.07	101.94	0.01
55	108.03	0.04	103.97	-0.01
56	109.86	0.04	105.95	0.01
57	111.87	0.03	107.96	0.03
58	113.91	0	109.95	0.03
59	115.93	0.01	111.96	0.01
60	118.02	0.01	113.96	0.04
61	119.97	0	115.95	0.03
62	121.98	0.08	117.94	0.03
63	123.86	0.02	119.96	0.03
64	126.05	0.07	121.97	0.04
65	127.94	0.05	123.95	0.04
66	129.97	0.05	125.95	0.01
67	131.95	0.01	127.99	0.01
68	133.9	0.01	129.98	0
69	135.87	0.04		
70	137.91	0.08		
71	139.92	0.12		
72	141.83	0.1		

Distances and elevations along seismic line Ray Chem 2.
Measurements are relative to first shotpoint.

Shot Number	Shot Dist. (m)	Shot Elev. (m)	Receiver Dist. (m)	Receiver Elev. (m)
1	0	0.16	24.01	0.07
2	2.04	0.08	26.06	0.02
3	3.91	0.19	28.09	0.13
4	5.98	0.19	30.01	0.02
5	7.96	0.16	32.03	-0.02
6	10.08	0.16	34.02	-0.03
7	12.07	0.15	35.97	-0.05
8	13.88	0.14	38.04	-0.04
9	15.88	0.12	40.11	0.01
10	17.88	0.1	42.04	-0.03
11	20.01	0.17	44.04	-0.02
12	21.94	0.13	46.05	-0.02
13	24.1	0.2	48.01	0.01
14	25.95	0.17	50.03	-0.03
15	27.87	0.13	52.03	-0.01
16	29.92	0.19	54.04	-0.01
17	31.91	0.15	56.01	0
18	33.88	0.18	58.02	0.01
19	35.9	0.13	60.02	0.03
20	37.94	0.08	62.04	0
21	39.95	0.13	64.03	-0.01
22	41.81	0.1	66.02	-0.02
23	43.88	0.12	68	0
24	45.85	0.14	70.02	-0.03
25	47.88	0.17	72.01	0.03
26	49.95	0.22	74.03	0.03
27	51.9	0.21	76.02	0.14
28	53.89	0.09	77.98	0.3
29	56.01	0.11	80.03	0
30	57.99	0.11	82	-0.02
31	59.96	0.12	84.04	0.02
32	61.91	0.12	86	0.03
33	63.91	0.12	87.98	0.15
34	65.91	0.12	89.99	-0.06
35	68.11	0.15	91.98	-0.03
36	70.09	0.11	94.01	-0.01
37	72.01	0.19	96.05	-0.05
38	73.99	0.17	98.05	-0.12
39	75.95	0.19	100.04	-0.04
40	77.95	0.18	102.05	-0.02
41	80.03	0.21	104.01	-0.05
42	81.96	0.18	106.04	-0.06

43	84.02	0.2	108.02	-0.04
44	85.98	0.12	110.03	-0.02
45	88.04	0.19	112	-0.08
46	90.04	0.2	114.04	-0.01
47	92.05	0.17	116.03	-0.02
48	94.05	0.13	118.03	0
49	96.07	0.14	120.03	-0.05
50	97.99	0.08	122.01	-0.07
51	99.97	0.06	124.03	-0.06
52	101.95	0.02	125.99	-0.04
53	103.93	0.03	128.01	-0.07
54	105.9	0.01	130.01	-0.04
55	107.93	0.05	131.99	-0.03
56	110.02	0.04	133.97	-0.07
57	111.95	0.08	135.99	-0.04
58	113.98	0.04	138	-0.05
59	115.97	0.06	140.03	0.09
60	118.07	0.06	142.06	0.18
61	119.98	0.06		
62	121.89	0		
63	123.98	0.05		
64	126.03	0.03		
65	127.92	0.07		
66	129.99	0		
67	131.95	0.05		
68	133.87	0		
69	135.92	0.04		
70	137.93	0.02		
71	139.98	0.15		
72	141.95	0.11		
73	143.97	0.08		
74	145.94	0.07		
75	148.01	0.04		
76	149.94	0.07		
77	152.08	0.1		
78	153.94	0.06		
79	156.05	0.08		
80	157.92	0.06		
81	160.03	0.12		
82	161.96	0.05		
83	163.94	0.11		
84	165.84	0.12		